



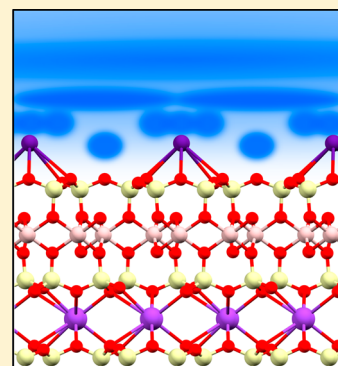
## Concentration-Dependent Adsorption of CsI at the Muscovite–Electrolyte Interface

Sander J.T. Brugman, Eleanor R. Townsend, Mireille M.H. Smets,<sup>1</sup> Paolo Accordini, and Elias Vlieg<sup>\*1</sup>

Radboud University, Institute for Molecules and Materials, Heyendaalseweg 135, 6525AJ Nijmegen, The Netherlands

### Supporting Information

**ABSTRACT:** The interfacial structure of muscovite in contact with aqueous CsI solutions was measured using surface X-ray diffraction for several CsI concentrations (2–1000 mM). At CsI concentrations up to 200 mM, Cs<sup>+</sup> adsorption is likely hindered by H<sub>3</sub>O<sup>+</sup>, as both cations compete for the adsorption site above the muscovite hexagonal cavity. Above this concentration, more Cs<sup>+</sup> adsorbs than is required to compensate the negatively charged muscovite surface, which means that coadsorption of an anion takes place. The I<sup>−</sup> anion does not coadsorb in an ordered manner. Moreover, the hydration ring and water layers do not change significantly as a function of the CsI concentration.



### ■ INTRODUCTION

Many processes such as corrosion, lubrication, adsorption of organic molecules, crystal growth, and catalysis take place at the interface between the solid and liquid state. While fundamental knowledge about the solid–liquid interface is desired, it is often difficult to access the interfacial structure. To investigate the interface, experimental techniques that can reach atomic resolution, measure in situ in solution, and do not interfere with the interface itself are required. Surface X-ray diffraction (SXRD) fulfils these criteria and is therefore often used to study interfaces. The muscovite mica surface in contact with an electrolyte solution has been extensively studied by SXRD<sup>1–3</sup> because of its flatness<sup>4</sup> and its similarity to clay minerals.

The muscovite structure [ideal formula KAl<sub>2</sub>(Si<sub>3</sub>Al)O<sub>10</sub>(OH)<sub>2</sub>] consists of one octahedral sheet in between two tetrahedral sheets. By isomorphous substitution, 25% of the Si atoms in the tetrahedral sheets are replaced by Al.<sup>5</sup> This gives rise to permanently negatively charged tetrahedral sheets, which are held together by a layer of K<sup>+</sup> ions. Muscovite can be cleaved in the (001) direction through this relatively weakly bound K<sup>+</sup> layer to form a flat and clean surface. It has been shown that by cleaving using a scalpel, large (>1 cm<sup>2</sup>) step-free areas can be created.<sup>4</sup> It is important to note that there are two crystallographically distinct surface terminations possible, which are interconnected via a glide plane. A more detailed explanation is given by Pintea et al.<sup>2</sup>

By submerging the cleaved surface in an electrolyte solution, the exposed surface K<sup>+</sup> ions can be exchanged for other cations.<sup>6,7</sup> The permanent negative charge of the muscovite surface is equal to 1e<sup>−</sup> per surface unit cell, that is, two adsorption sites. Therefore, the surface charge is exactly compensated at a monovalent cation occupancy of 50%. Although in SXRD experiments, a cation occupancy close to

50% has been observed,<sup>2</sup> atomic force microscopy (AFM) measurements surprisingly found a fully covered muscovite surface (i.e., occupancy of 100%).<sup>8</sup> In view of charge neutrality, an occupancy higher than 50% is possible, but requires compensation of the excess positive charge. One possibility to achieve charge neutrality is by coadsorption of an anion to the surface. In some literature, evidence was found for coadsorption of Cl<sup>−</sup>.<sup>2,9,10</sup> By contrast, Sakuma et al. found that for a KI electrolyte solution, no coadsorption of I<sup>−</sup> takes place at the muscovite interface.<sup>11</sup>

The aim of this work is to determine the effect of the electrolyte concentration on the charge balance on the surface. CsI was chosen as the electrolyte because of the strong X-ray scattering of the Cs<sup>+</sup> and I<sup>−</sup> ions, which facilitates detection. Previously, X-ray reflectivity measurements showed that the Cs<sup>+</sup> adsorption on the muscovite surface was different for 10 and 500 mM CsCl solutions.<sup>12</sup> Therefore, multiple concentrations between 2 and 1000 mM CsI were measured to investigate how the Cs<sup>+</sup> occupancy relates to the CsI concentration. Moreover, the role of the I<sup>−</sup> anion in the charge balance of the muscovite surface is investigated.

### ■ EXPERIMENTAL SECTION

**Materials.** High-quality muscovite mica sheets (ASTM-V1 quality grade, S&J Trading Inc. Glen Oaks, NY, USA) were cut into pieces of approximately 45 × 45 mm<sup>2</sup> using scissors and were freshly cleaved in the (001) direction using a scalpel. Immediately after cleavage, the muscovite was submerged in aqueous CsI (Aldrich, 99.9% pure) solution of different CsI concentrations (2–1000 mM) for the

**Received:** January 5, 2018

**Revised:** February 13, 2018

**Published:** March 9, 2018



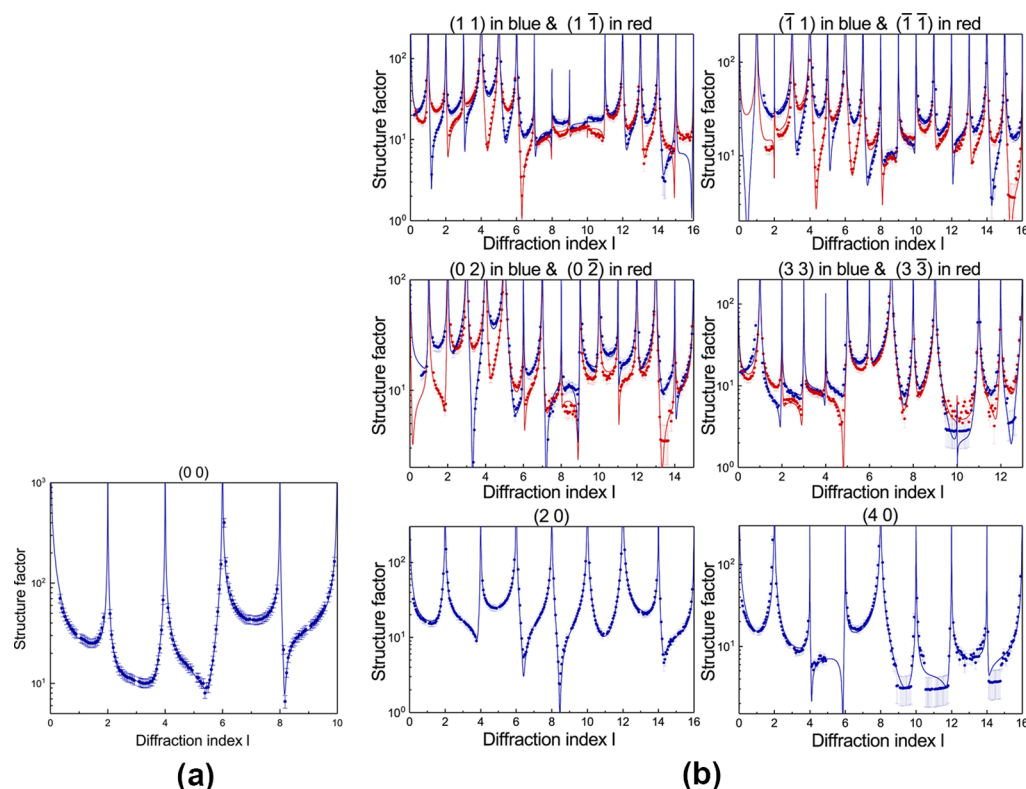


**Figure 1.** Experimental (a) specular and (b) nonspecular crystal truncation rods (symbols with error bars) for muscovite in contact with 500 mM CsI solution. The best model fit is shown as a solid line; see text.

exchange of surface ions. The pH of the solution was approximately around 6 for all concentrations, as was indicated by the indicator paper; because using a pH meter, no stable pH value could be obtained. The pH was not adjusted. Muscovite was kept in solution for at least 30 min. Subsequently, the sample was placed on a metal sample holder. Some additional drops of solution were added on top of the sample and in the sample cell to prevent evaporation of the liquid film and to maintain a stable environment. The cell was covered by a Mylar foil (13  $\mu\text{m}$ , Lebow Company, Goleta, CA, USA). Excess liquid on top of the sample was removed by gently wiping a tissue over the Mylar foil. For each CsI concentration, a new piece of muscovite was used.

**SXRD.** In an SXRD experiment, the diffracted intensity is measured at different positions in reciprocal space. This diffracted intensity is the square of the structure factor, which contains the desired structural information. The structure factor of an interface is composed of a contribution of the bulk crystal and a contribution of the interface, which can simply be added to obtain the total structure factor:  $F_{hkl}^{\text{total}} = F_{hkl}^{\text{bulk}} + F_{hkl}^{\text{interface}}$ . Because the contribution of the bulk to the structure factor is about  $10^6$  times more intense than the interface contribution to the structure factor, synchrotron radiation is required to obtain enough intensity from the weakly scattering surface. Using SXRD, it is possible to obtain the interface structure with (sub)atomic resolution. Unlike for AFM, where individual unit cells can be imaged, in SXRD, the interface structure is averaged over a large amount of unit cells, depending of the footprint of the X-ray beam. Diffracted signal originates only from ordered, that is, the crystalline parts of the interface. Therefore, if solvent molecules exhibit some order close to the surface, this is reflected in the measurement.<sup>13</sup> Because the diffracted intensity scales with the electron density, heavier atoms give rise to a stronger signal. This means that elements with a low atomic number can be difficult to observe. Especially hydrogen is nearly invisible to X-rays.

**Data Acquisition and Analysis.** SXRD measurements were conducted at the ID03 beam line of the European Synchrotron Radiation Facility (ESRF) on a vertical  $z$ -axis type geometry

diffractometer using a MAXIPIX area detector in stationary geometry for CsI concentrations up to 200 mM. A beam size of  $340 \times 28 \mu\text{m}^2$  (horizontal  $\times$  vertical) was selected. SXRD measurements for the two highest CsI concentrations (500 and 1000 mM) were conducted on a vertical (2 + 2)-type diffractometer at the I07 beam line of the Diamond Light Source, using a Pilatus 100 K area detector in stationary geometry. For these experiments, a beam size of  $200 \times 100 \mu\text{m}^2$  was chosen. For all experiments, an X-ray energy of 20 keV was used. In the experiments, the diffracted intensity was measured as a function of the momentum transfer  $Q = h\vec{a}^* + k\vec{b}^* + l\vec{c}^*$ , where  $\vec{a}^*$ ,  $\vec{b}^*$ , and  $\vec{c}^*$  denote the reciprocal lattice vectors and  $(hkl)$  denotes the diffraction indices. For nonspecular crystal truncation rods, a constant angle of incidence of  $0.6^\circ$  was used. The surface of muscovite was scanned by measuring the (1 1 1.3) reflection to select a step-free area [see the Supporting Information (S1)]. For most concentrations, the (0 0), (1 1), (1  $\bar{1}$ ), ( $\bar{1}$  1), ( $\bar{1}$   $\bar{1}$ ), (1 3), (1  $\bar{3}$ ), (3 3), (3  $\bar{3}$ ), (0 2), (0  $\bar{2}$ ), (2 0), and (4 0) crystal truncation rods were measured. A number of crystal truncation rods were measured at the start of the experiment and measured again after a few hours and did not show any differences, indicating that the X-ray beam has no significant effect in our geometry. Moreover, consistent results were obtained for many samples and two different synchrotrons, showing the reproducibility of the results.

Because only one surface termination of muscovite is present in the measurements, it is not possible to estimate the systematic error from symmetry equivalent reflections.<sup>2</sup> For all data sets, an error of 10% was assumed. To increase the importance of the specular rod in the analysis, the weight factor for this crystal truncation rod was multiplied by a factor of 5. Data points close to a Bragg peak were given a 30% larger error to increase the relative weight of surface sensitive data points. A MATLAB script ("ARTS") was used to convert the integrated intensities into structure factors. Although the standard correction factors<sup>14</sup> put all data on the same scale, it was found that an improved fit was obtained when each crystal truncation rod was given an independent scale factor. This is most likely because of inhomogeneities in the illuminated sample area and absorption by

Table 1. Structural Parameters of Muscovite in Contact with Aqueous 500 mM CsI Solution<sup>a</sup>

element	z-height (Å)	occupancy (%)	in-plane vibration (Å)	out-of-plane vibration (Å)
water <sub>third layer</sub>	8.7 ± 0.4	790 ± 40	∞	6.3 ± 0.4
water <sub>second layer</sub>	5.4 ± 0.3	140 ± 30	∞	1.2 ± 0.4
water <sub>first layer</sub>	4.6 ± 0.1	72 ± 5	2.5 ± 0.4	0.1 ± 0.1
hydration ring	3.70 ± 0.10	17 ± 20	0.32 ± 0.05	0.79 ± 0.05
Cs <sub>cavity</sub> <sup>+</sup>	2.16 ± 0.05	62 ± 5	0.24 ± 0.05	0.21 ± 0.05
water & H <sub>3</sub> O <sub>cavity</sub> <sup>+</sup>	2.04 ± 0.05	38 ± 5	0.21 ± 0.05	0.10 ± 0.05
O <sub>bulk,top</sub>	0	100 (fixed)	0.12 ± 0.05	0.20 ± 0.05
Si/Al	−0.59 ± 0.05	100 (fixed)	0.10 ± 0.05	0.12 ± 0.05

<sup>a</sup>The average position of the topmost oxygen atoms of the muscovite structure is defined as 0 in the z-direction

the liquid. The ROD software was used to fit the surface structure to the measured data.<sup>15</sup> The possibility to add a uniform liquid layer was implemented in the ROD software to incorporate the electrolyte layer on top of muscovite. Atomic scattering coefficients<sup>16</sup> and anomalous scattering coefficients<sup>17</sup> at 20 keV were used. The replacement of 25% of Si by Al in the muscovite bulk was taken into account in these values. Unit cell parameters ( $C2/c$ ,  $a = 5.1906$  Å,  $b = 9.0080$  Å,  $c = 20.0470$  Å, and  $\beta = 95.757^\circ$ ) and atomic positions of muscovite bulk crystal structure were obtained from Güven.<sup>18</sup>

## RESULTS AND DISCUSSION

**Liquid Layer Thickness.** To correct for absorption of the X-ray beam, an estimation of the thickness of the liquid layer on top of muscovite is necessary. For this purpose, the (1 3) crystal truncation rod of muscovite in contact with 50 mM KI (Sigma, ≥99.5% pure) was measured three times with incident angles of 0.3, 0.6, and 1.2°. In all cases, the absorption was different because of the difference in the path lengths through the Mylar foil and the solution layer. The transmission is given by  $T = T_{\perp}^{1/\sin\beta_{in}} \times T_{\perp}^{1/\sin\beta_{out}}$ , where  $T_{\perp}$  is the transmission perpendicular through the film and  $\beta_{in}$  and  $\beta_{out}$  are the angle of incidence and the outgoing angle, respectively. For values of  $l$  that are high enough, that is, a large  $\beta_{out}$  angle, the transmission of the outgoing beam is very close to 1, and in addition, will be nearly identical for all three incoming angles. Experimentally, the ratio of  $T_{0.6^\circ}/T_{1.2^\circ}$  and  $T_{0.3^\circ}/T_{1.2^\circ}$  was determined. For  $2 \geq l \geq 4.5$ , this gave an average perpendicular transmission  $T_{\perp}$  of  $0.9992 \pm 0.0001$ . This experimental transmission is already lower than the theoretical transmission through a 13 μm Mylar foil, which is 0.9991 at 20 keV.<sup>19</sup> This means that the liquid film on top of muscovite is very thin. For comparison, the transmission through 3 μm of water is 0.9998. Within the errors of the experiment, the liquid film cannot be much thicker than this 3 μm. Nevertheless, this is much thicker than the liquid layer above the muscovite surface exhibiting some order, which is about 1 nm.<sup>2</sup> For the absorption correction, a  $T_{\perp}$  value of 0.9992 was used for all experiments.

**Interface Model.** Using SXRD, the muscovite (001) surface was measured in contact with an aqueous CsI solution of different concentrations. Solutions of 2, 10, 50, 200, 500, and 1000 mM CsI were used. For all concentrations, the specular and at least 10 nonspecular crystal truncation rods were acquired. Figure 1 shows the measured crystal truncation rods for muscovite in contact with 500 mM CsI solution. The measured crystal truncation rods for the other CsI concentrations can be found in the Supporting Information (S2).

A structural model was made to fit the measured crystal truncation rods, using  $\chi^2$  as the goodness-of-fit criterion.<sup>20</sup> The best model was defined as the model with the lowest reduced  $\chi^2$  value. If the introduction of a new feature to the model did not lower the reduced  $\chi^2$  value significantly, it was rejected. The

best fit (solid line in Figure 1) was achieved with a model similar to that of Pintea et al.<sup>2</sup> The structural parameters derived from the best fit are shown in Table 1 and visualized in Figure 2 for the case of muscovite in contact with 500 mM CsI

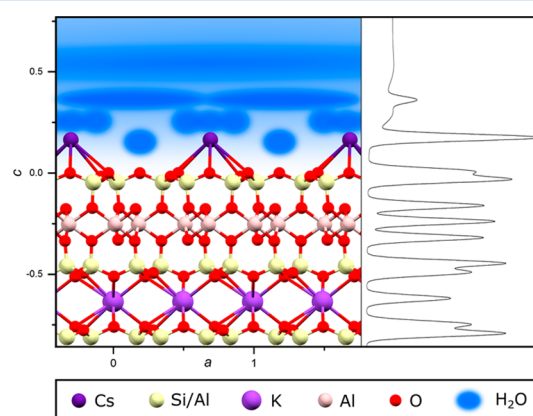
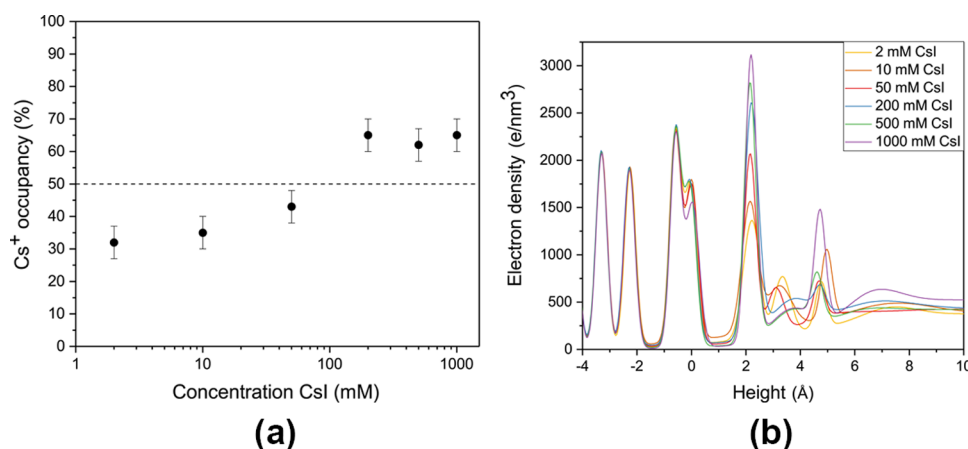


Figure 2. Illustration of the model of the interfacial structure of muscovite in contact with aqueous CsI solution. The right part of the figure shows the projected electron density for muscovite in contact with 500 mM CsI solution.

solution. In short, the best model consists of a fixed bulk muscovite region, a “flexible” crystalline region, an interface region, and a bulk liquid region. The “flexible” crystalline region contains four layers (Al, O, Si/Al, and O) with an occupancy of 100%, of which all atoms were free to move vertically. Horizontal displacements are not expected for these atoms and are incorporated in the in-plane vibration parameters. A larger “flexible” region was tested, but did not yield a better fit. The interface region consists of (1) Cs<sup>+</sup> and O adsorbed above the center of the muscovite hexagonal cavity, (2) a hydration ring with a radius of  $2.7 \pm 0.3$  Å above Cs<sup>+</sup>, and (3) three water layers without lateral ordering. The hydration ring was modelled as 12 oxygen atoms at an equal distance from the Cs<sup>+</sup> ion. In the interface layer, all atoms were allowed to move in the horizontal and vertical directions. Additionally, the occupancy and the in-plane and out-of-plane vibration parameters were allowed to vary. Any partial ordering in the interface region was modelled by anisotropic Debye–Waller parameters. The Debye–Waller parameter relates to the mean-square thermal vibration amplitude  $\langle u^2 \rangle$  by  $B = 8\pi^2\langle u^2 \rangle$ .<sup>13,20</sup> Because of the insensitivity of X-rays to H, water was modelled as a single O atom in all models. Because the space above the hexagonal cavity has to be filled with either water or Cs<sup>+</sup>, a constraint has been added that the total Cs<sup>+</sup> and O occupancy directly above the cavity should equal 1. Fits performed without this constraint led to a similar goodness-of-fit and nearly





**Figure 3.** (a) Occupancy of adsorbed  $\text{Cs}^+$  on the muscovite surface as a function of the CsI concentration. The dashed line indicates the expected occupancy of  $\text{Cs}^+$  corresponding to charge neutrality. (b) Electron density perpendicular to the surface for different CsI concentrations.

identical  $\text{Cs}^+$  occupancies. The addition of an extra adsorption site above the surface Si/Al atoms did not yield a better fit. The bulk liquid region was modelled by a continuous layer with the density of the salt solution, where the starting height and interface width were fitting parameters. Good fits for all CsI concentrations were obtained using the same structural model. For the 500 mM CsI data, the  $\chi^2$  value obtained was 0.91.

**Comparison of Different CsI Concentrations.** When the structural parameters of all CsI concentrations [Supporting Information (S2)] were compared, the most striking difference was found in the  $\text{Cs}^+$  adsorption. Figure 3a shows the adsorbed  $\text{Cs}^+$  occupancy as a function of the CsI concentration in solution. In Figure 3b, the full electron density profile in the out-of-plane direction is shown, in which the increase in the  $\text{Cs}^+$  occupancy as a function of the concentration can be seen as an increase in the electron density at a height of  $2.17 \pm 0.03$  Å above the average height of the top oxygen layer. At 2 and 10 mM CsI, about 34% of the adsorption sites are occupied by  $\text{Cs}^+$ , whereas at 200, 500, and 1000 mM, about 64% of the adsorption sites are occupied by  $\text{Cs}^+$ . The 50 mM CsI concentration is an intermediate case with an adsorption site  $\text{Cs}^+$  occupancy of  $43 \pm 5\%$ . The significance of the difference in  $\text{Cs}^+$  adsorption at low and high concentrations is described in the Supporting Information (S3).

At the two lowest concentrations, only about 70% of the negative surface charge of muscovite is compensated by  $\text{Cs}^+$ , which corresponds to an uncompensated charge of approximately  $0.35 \text{ e}^-/\text{nm}^2$ . This is an order of magnitude higher than the charge that is expected to be compensated in the diffuse layer derived from zeta potential measurements.<sup>21</sup> This means that, to achieve charge neutrality, another positively charged species should be present on the surface.  $\text{Cs}^+$  is assumed to adsorb strongly in an inner-sphere configuration,<sup>22,23</sup> and because no other cations are present except hydronium, it can be concluded that the residual charge is compensated by  $\text{H}_3\text{O}^+$ . This is remarkable because the  $\text{H}_3\text{O}^+$  concentration is only about  $1 \mu\text{M}$ , which is much lower than the  $\text{Cs}^+$  concentrations of 2 or 10 mM, where  $\text{H}_3\text{O}^+$  has a large impact. This means that the affinity of muscovite for hydronium is much higher than for  $\text{Cs}^+$ , which has been seen in previous experiments.<sup>24–27</sup> Note that in our SXRD experiments,  $\text{H}_3\text{O}^+$  cannot be observed directly because it has the same X-ray characteristics as  $\text{H}_2\text{O}$  (or O). The only other positive ion that could play a role is  $\text{K}^+$ , which is initially present at the cleaved muscovite surface.

However, the  $\text{K}^+$  ions are expected to be fully exchanged for  $\text{Cs}^+$ .<sup>27,28</sup> The concentration of the  $\text{K}^+$  surface ions is of the order of  $\mu\text{M}$  when put in the 50 mM CsI solution during the ion-exchange step, which is low compared to the CsI concentration. Moreover, considering that the difference in the adsorption free energy (i.e., affinity to the surface) between  $\text{Cs}^+$  and  $\text{K}^+$  is small, it is expected that  $\text{K}^+$  will not remain on the surface during the ion-exchange step and therefore does not play a role in this experiment.<sup>3,22,29</sup>

For CsI concentrations above 200 mM, about 130% of the surface charge is compensated, that is, a 30% overcompensation. To maintain charge neutrality, negative ions with an occupancy of about 15% should be present near the interface. Using SXRD, such ions are only observed if they show sufficient order. We found sharp peaks in the electron density at a height of  $4.8 \pm 0.1$  Å (see Figure 3b), which is a possible location for the negative ions. The electron density at this location also shows lateral ordering. Previously, for muscovite in contact with 56 mM CsCl solution, a similar peak was observed and was attributed to coadsorption of  $\text{Cl}^-$  with an occupancy of  $25\% \pm 10\%$ .<sup>2</sup> In our case, the peak in the electron density could correspond to an  $\text{I}^-$  occupancy of  $10 \pm 8\%$ . A closer comparison between the 56 mM CsCl and 50 mM CsI solutions (Figure 4) shows that the electron density at the peak position is similar, whereas a density peak from  $\text{I}^-$  should be about 3 times higher than the one from  $\text{Cl}^-$  with the same

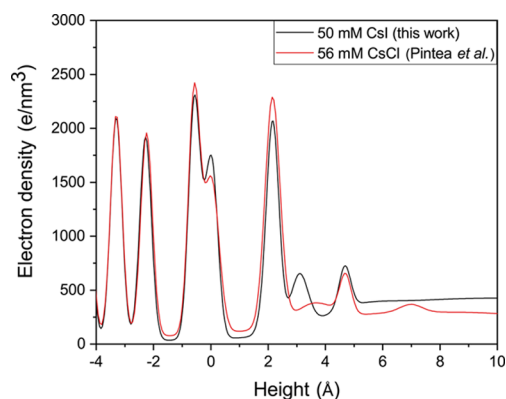


**Figure 4.** Electron density perpendicular to the surface of muscovite in contact with 50 mM CsI solution compared to 56 mM CsCl solution measured by Pintea et al.<sup>2</sup>

occupancy. This makes it unlikely that the density peak is caused by  $\text{I}^-$  (or  $\text{Cl}^-$ ), which is in corroboration with an X-ray reflectivity study in which KI adsorption on the muscovite surface was compared to KCl adsorption.<sup>11</sup> This suggests that in both cases, the electron density has a common origin. A possible candidate is  $\text{OH}^-$ , which should be present with an occupancy of about 15% for charge compensation. The remainder of the peak electron density would then be  $\text{H}_2\text{O}$ . The charge-compensating role of  $\text{OH}^-$  would lead to a strong order in the entire layer. Unfortunately, SXRD cannot distinguish the two species  $\text{OH}^-$  and  $\text{H}_2\text{O}$  or even a mixture with small amounts of  $\text{I}^-$  (<10%). At a pH of approximately 6, the  $\text{OH}^-$  concentration is very low, but this does not exclude a much higher density at the interface. As our measurements do not indicate that the  $\text{I}^-$  anion is present at the interface in an ordered position, it is expected that the results are independent of the type of anion.

Purely based on electron density,  $\text{Cs}^+$  also could be located at a height of  $4.8 \pm 0.1 \text{ \AA}$  with an occupancy of  $10 \pm 8\%$ ; however, this would only make the charge overcompensation worse. Moreover, as mentioned before,  $\text{Cs}^+$  has been reported to adsorb strongly in an inner-sphere configuration.<sup>22</sup>

Given our observation that the maximum coverage of  $\text{Cs}^+$  is approximately 64%, it is possible that the same charge overcompensation occurs at a low  $\text{Cs}^+$  concentration but then through the combination of  $\text{Cs}^+$  and  $\text{H}_3\text{O}^+$  ions. Roughly speaking, the  $\text{Cs}^+$  adsorption is found to increase from one to two out of every three hexagonal adsorption sites. If the charge in this layer was indeed constant, the  $\text{H}_3\text{O}^+$  adsorption would decrease from one to zero per three adsorption sites for increasing  $\text{Cs}^+$  concentration. The third site would have a constant occupancy of  $\text{H}_2\text{O}$ . In this speculative scenario, the anion would have a constant occupancy of 15% in the  $\text{H}_2\text{O}/\text{OH}^-$  layer at a height of  $4.8 \pm 0.1 \text{ \AA}$  for all CsI concentrations. It is also possible that the excess positive charge is compensated by diffuse  $\text{OH}^-$  or  $\text{I}^-$  anions with the same occupancy.

The three-site scenario suggests some (local) ordering, for which SXRD is not sensitive. Such ordering was proposed to occur based on AFM measurements of  $\text{Rb}^+$  and  $\text{K}^+$  adsorption.<sup>8,30</sup> In their AFM measurements, Ricci et al. found a  $\text{Rb}^+$  occupancy of 100% at a concentration of 10 mM  $\text{RbCl}$ .<sup>8</sup> They explained this observation by the existence of alternating patches with 100%  $\text{Rb}^+$  occupancy and patches with 0%  $\text{Rb}^+$  occupancy, which would fulfil charge neutrality. Our measurements show that the  $\text{Cs}^+$  occupancy does not reach 100% at high CsI concentrations. The measured structure factors are averaged over a large amount of unit cells; therefore, SXRD is inherently insensitive for the existence of these patches. On the other hand, Martin-Jimenez and Garcia found a  $\text{K}^+$  occupancy of 50% at 200 mM KCl concentration using AFM, which fulfils charge neutrality and is in line with the SXRD results.<sup>2,30</sup>

For all CsI concentrations,  $\text{Cs}^+$  adsorbs above the center of the hexagonal cavity at a height of  $0.46 \pm 0.03 \text{ \AA}$  above the bulk K position, which is in good agreement with the literature.<sup>1–3,9,12,29</sup> The lateral displacement of  $\text{Cs}^+$  is in all cases smaller than the in-plane vibration parameter. The height of  $\text{Cs}^+$  is nearly constant for all independent fits [see Supporting Information (S4)], demonstrating the accuracy in the determination of this parameter. Pintea et al. found that the  $\text{Cs}^+$  occupancy was  $57 \pm 10\%$  per surface unit cell at a concentration of 56 mM  $\text{CsCl}$ , which is close to the value of  $43 \pm 5\%$  found in this work at a concentration of 50 mM  $\text{CsI}$ .<sup>2</sup> Both concentrations lie in the transition region from a low to a

high  $\text{Cs}^+$  occupancy, which might explain the small discrepancy between the occupancies.

The hydration ring shows a small increase in the occupancy for CsI concentrations of 200 mM and above [Supporting Information (S4)]. Because this hydration ring is attributed to  $\text{Cs}^+$ , the increase in the occupancy of the hydration ring can be explained by the observed increase of the  $\text{Cs}^+$  occupancy. Moreover, the height and out-of-plane vibration of this hydration ring increase at CsI concentrations of 200 mM and above, but the cause of this increase is unclear. The height, occupancy, in-plane vibration, and out-of-plane vibration of the water layers do not show a clear trend when the CsI concentration is altered, as can be seen in Figure 3b and in the Supporting Information (S4). For the aim of this paper, these details are not important.

## CONCLUSIONS

Using SXRD, the specular and several nonspecular crystal truncation rods of the muscovite basal plane in contact with different concentrations of aqueous CsI were measured. An interface model was proposed, which gave good fits for all measured CsI concentrations.

At low CsI concentrations, the  $\text{Cs}^+$  adsorption does not fully compensate the muscovite negative charge, implying the adsorption of  $\text{H}_3\text{O}^+$ . On the other hand, at high CsI concentrations, the muscovite negative charge is overcompensated by  $\text{Cs}^+$ , which can only be explained by the coadsorption of anions. In this case, the only anions present are  $\text{I}^-$  and to a lesser extend  $\text{OH}^-$ . A comparison with the results on  $\text{CsCl}$  obtained by Pintea et al. showed that  $\text{I}^-$  does not coadsorb in an ordered manner.

This work shows that the cation adsorption on the muscovite surface is concentration dependent, up to relatively high concentrations of about 200 mM CsI, and that competition with  $\text{H}_3\text{O}^+$  plays a significant role in  $\text{Cs}^+$  adsorption. Moreover, it shows that the coadsorption of anions should be considered in (theoretical) models describing the surface. Complementary simulation studies could aid in explaining why the  $\text{Cs}^+$  adsorption levels off at an occupancy of about 64% at high CsI concentrations.

## ASSOCIATED CONTENT

### Supporting Information

The Supporting Information is available free of charge on the ACS Publications website at DOI: 10.1021/acs.langmuir.8b00038.

Identification of the surface terminations, measured crystal truncation rods, accuracy of the  $\text{Cs}^+$  occupancy, and structural parameters (PDF)

## AUTHOR INFORMATION

### Corresponding Author

\*E-mail: e.vlieg@science.ru.nl

### ORCID

Mireille M.H. Smets: 0000-0003-1938-2099

Elias Vlieg: 0000-0002-1343-4102

### Notes

The authors declare no competing financial interest.

## ACKNOWLEDGMENTS

This work is part of the Industrial Partnership Programme Rock-on-a-Chip that is carried out under an agreement between BP Exploration Operating Company Limited and the Netherlands Organisation for Scientific Research (NWO). The experiments were performed on beamline ID03 at the ESRF, Grenoble, France and on beamline I07 at the Diamond Light Source, Didcot, United Kingdom. We are grateful to Maciej Jankowski at the ESRF and Jonathan Rawle at the Diamond Light Source for providing assistance in using these beamlines.

## REFERENCES

- (1) Lee, S. S.; Fenter, P.; Nagy, K. L.; Sturchio, N. C. Monovalent ion adsorption at the muscovite (001)–solution interface: Relationships among ion coverage and speciation, interfacial water structure, and substrate relaxation. *Langmuir* **2012**, *28*, 8637–8650.
- (2) Pintea, S.; de Poel, W.; de Jong, A. E. F.; Vonk, V.; van der Asdonk, P.; Drnec, J.; Balmes, O.; Isern, H.; Dufrane, T.; Felici, R.; Vlieg, E. Solid-Liquid Interface Structure of Muscovite Mica in CsCl and RbBr Solutions. *Langmuir* **2016**, *32*, 12955–12965.
- (3) Bourg, I. C.; Lee, S. S.; Fenter, P.; Tournassat, C. Stern Layer Structure and Energetics at Mica–Water Interfaces. *J. Phys. Chem. C* **2017**, *121*, 9402–9412.
- (4) de Poel, W.; Pintea, S.; Drnec, J.; Carla, F.; Felici, R.; Mulder, P.; Elemans, J. A. A. W.; van Enckevort, W. J. P.; Rowan, A. E.; Vlieg, E. Muscovite mica: Flatter than a pancake. *Surf. Sci.* **2014**, *619*, 19–24.
- (5) Bragg, W. L. *Atomic structure of minerals*; Cornell University Press, 1937.
- (6) Gaines, G. L., Jr. The ion-exchange properties of muscovite mica. *J. Phys. Chem.* **1957**, *61*, 1408–1413.
- (7) de Poel, W.; Vaessen, S. L.; Drnec, J.; Engwerda, A. H. J.; Townsend, E. R.; Pintea, S.; de Jong, A. E. F.; Jankowski, M.; Carla, F.; Felici, R.; Elemans, J. A. A. W.; van Enckevort, W. J. P.; Rowan, A. E.; Vlieg, E. Metal ion-exchange on the muscovite mica surface. *Surf. Sci.* **2017**, *665*, 56–61.
- (8) Ricci, M.; Spijker, P.; Voitchovsky, K. Water-induced correlation between single ions imaged at the solid–liquid interface. *Nat. Commun.* **2014**, *5*, 4400.
- (9) Sakuma, H.; Kawamura, K. Structure and dynamics of water on Li<sup>+</sup>, Na<sup>+</sup>, K<sup>+</sup>, Cs<sup>+</sup>, H<sub>3</sub>O<sup>+</sup>-exchanged muscovite surfaces: a molecular dynamics study. *Geochim. Cosmochim. Acta* **2011**, *75*, 63–81.
- (10) Meleshyn, A. Aqueous solution structure at the cleaved mica surface: Influence of K<sup>+</sup>, H<sub>3</sub>O<sup>+</sup>, and Cs<sup>+</sup> adsorption. *J. Phys. Chem. C* **2008**, *112*, 20018–20026.
- (11) Sakuma, H.; Nakao, H.; Yamasaki, Y.; Kawamura, K. Structure of Electrical Double Layer at Mica/KI Solution Interface. *J. Appl. Solution Chem. Model.* **2012**, *1*, 1–5.
- (12) Schlegel, M. L.; Nagy, K. L.; Fenter, P.; Cheng, L.; Sturchio, N. C.; Jacobsen, S. D. Cation sorption on the muscovite (001) surface in chloride solutions using high-resolution X-ray reflectivity. *Geochim. Cosmochim. Acta* **2006**, *70*, 3549–3565.
- (13) Reedijk, M. F.; Arsic, J.; Hollander, F. F. A.; De Vries, S. A.; Vlieg, E. Liquid order at the interface of KDP crystals with water: Evidence for icelike layers. *Phys. Rev. Lett.* **2003**, *90*, 066103.
- (14) Vlieg, E. Integrated intensities using a six-circle surface x-ray diffractometer. *J. Appl. Crystallogr.* **1997**, *30*, 532–543.
- (15) Vlieg, E. ROD: a program for surface X-ray crystallography. *J. Appl. Crystallogr.* **2000**, *33*, 401–405.
- (16) *International Tables for Crystallography*; Prince, E., Ed.; Kluwer Academic Publishers, 2004; Vol. C.
- (17) Cromer, D. T.; Liberman, D. A. Anomalous dispersion calculations near to and on the long-wavelength side of an absorption edge. *Acta Crystallogr., Sect. A: Cryst. Phys., Diff., Theor. Gen. Crystallogr.* **1981**, *37*, 267–268.
- (18) Güven, N. The crystal structures of 2 M1 phengite and 2 M1 muscovite. *Z. Kristallogr.* **1971**, *134*, 196–212.
- (19) Henke, B. L.; Gullikson, E. M.; Davis, J. C. X-ray interactions: photoabsorption, scattering, transmission, and reflection at E= 50–30,000 eV, Z= 1–92. *At. Data Nucl. Data Tables* **1993**, *54*, 181–342.
- (20) Vlieg, E. In *Surface and Interface Science, Volume 1, Concepts and Methods*; Wandelt, K., Ed.; Wiley, 2012.
- (21) Scales, P. J.; Grieser, F.; Healy, T. W. Electrokinetics of the muscovite mica-aqueous solution interface. *Langmuir* **1990**, *6*, 582–589.
- (22) Lee, S. S.; Fenter, P.; Nagy, K. L.; Sturchio, N. C. Changes in adsorption free energy and speciation during competitive adsorption between monovalent cations at the muscovite (001)–water interface. *Geochim. Cosmochim. Acta* **2013**, *123*, 416–426.
- (23) Kerisit, S.; Okumura, M.; Rosso, K. M.; Machida, M. Molecular simulation of cesium adsorption at the basal surface of phyllosilicate minerals. *Clays Clay Miner.* **2016**, *64*, 389–400.
- (24) Pashley, R. M. DLVO and hydration forces between mica surfaces in Li<sup>+</sup>, Na<sup>+</sup>, K<sup>+</sup>, and Cs<sup>+</sup> electrolyte solutions: A correlation of double-layer and hydration forces with surface cation exchange properties. *J. Colloid Interface Sci.* **1981**, *83*, 531–546.
- (25) Pashley, R. M. Hydration forces between mica surfaces in electrolyte solutions. *Adv. Colloid Interface Sci.* **1982**, *16*, 57–62.
- (26) Pashley, R. M.; Israelachvili, J. N. DLVO and hydration forces between mica surfaces in Mg<sup>2+</sup>, Ca<sup>2+</sup>, Sr<sup>2+</sup>, and Ba<sup>2+</sup> chloride solutions. *J. Colloid Interface Sci.* **1984**, *97*, 446–455.
- (27) Park, C.; Fenter, P. A.; Sturchio, N. C.; Nagy, K. L. Thermodynamics, interfacial structure, and pH hysteresis of Rb<sup>+</sup> and Sr<sup>2+</sup> adsorption at the muscovite (001)–solution interface. *Langmuir* **2008**, *24*, 13993–14004.
- (28) Pashley, R. M. Hydration forces between mica surfaces in aqueous electrolyte solutions. *J. Colloid Interface Sci.* **1981**, *80*, 153–162.
- (29) Kobayashi, K.; Liang, Y.; Murata, S.; Matsuoaka, T.; Takahashi, S.; Nishi, N.; Sakka, T. Ion Distribution and Hydration Structure in the Stern Layer on Muscovite Surface. *Langmuir* **2017**, *33*, 3892–3899.
- (30) Martin-Jimenez, D.; Garcia, R. Identification of Single Adsorbed Cations on Mica–Liquid Interfaces by 3D Force Microscopy. *J. Phys. Chem. Lett.* **2017**, *8*, 5707–5711.